Light transmittance in forest canopies determined using airborne laser altimetry and in-canopy quantum measurements

Geoffrey G. Parker[a,*], Michael A. Lefsky[b,1], David J. Harding[c,2]

[a]*Smithsonian Environmental Research Center, P.O. Box 28, Edgewater, MD 21037, USA*
[b]*Pacific Northwest Experiment Station, 3200 SW Jefferson Way, Corvallis, OR 97331, USA*
[c]*Laboratory for Terrestrial Physics, NASA's Goddard Space Flight Center, Greenbelt, MD 20771, USA*

Abstract

The vertical distribution of light transmittance was derived from field and laser altimeter observations taken in the same canopies of five forests of several ages (young to mature) and canopy types (eastern broadleaved and western tall conifer). Vertical transmittances were derived remotely from the Scanning Lidar Imager of Canopies by Echo Recovery (SLICER) laser altimeter and in the field from measurements of Photosynthetically Active Radiation (PAR) made within the canopy using quantum sensors suspended from the gondola of a tower crane or atop small balloons. Derived numerical characteristics of mean transmittance profiles (the rate of attenuation, whole canopy transmittance, and the radiation-effective height) were similar for both methods across the sites. Measures of the variance and skewness of transmittance also showed similar patterns for corresponding heights between methods. The two methods exhibited greater correspondence in the eastern stands than in the western ones; differences in the interaction between canopy organization and the sensor characteristics between the stand types might explain this. The narrower, more isolated crowns of the western stands permit a deeper penetration into the canopy of nadir-directed laser light than of direct solar radiation from typical elevation angles. Transects of light transmittance in two stands demonstrate that the SLICER sensor can capture meaningful functional variation. Additionally, for one stand with numerous overlapping transects we constructed a three-dimensional view of the transmittance field. Using geostatistics, we demonstrated that the spatial covariance measured in the horizontal plane varied as a function of height. These results suggest a means to remotely assess an important functional characteristic of vegetation, providing a capacity for process-based ecological studies at large scales. © 2001 Elsevier Science Inc. All rights reserved.

1. Introduction

In vegetation canopies, the pattern of light transmittance indicates where radiation is absorbed, where carbon dioxide and water vapor are exchanged, and where leaves contain high levels of nutrients (Field & Mooney, 1986). Radiation interception is fundamental to canopy energy balance, influencing leaf and soil temperature and evaporation, and stand microclimate generally (Gutschick, 1991). The region of greatest change in transmittance is the "active" zone of the canopy. Characteristic features of this zone (gradient, location, and thickness) can indicate the developmental stage of the ecosystem, the stand-level intensity of competition for light, and the potential for growth (Parker, 1995). Ignorance of these characteristics limits the predictability of canopy function.

However, it is difficult to measure the canopy light environment, because access is challenging and the spatial and temporal variability of light is extreme. Direct observations of canopy light patterns have recently become available. Initial attempts used limited sampling from individual trees (Yoda, 1978), masts (Ellsworth & Reich, 1993; Thompson & Hinckley, 1977), or towers (Vose, Sullivan, Clinton, & Bolstad, 1995). Recent attempts, using balloons (Parker, Stone, & Bowers, 1996) or construction cranes (Parker, Smith, & Hogan, 1992), have been more extensive and spatially detailed. However, direct sampling within canopies has fundamental limitations: access by sensors requires insertion of a carrying system (e.g., balloon, personnel hoist, gondola), which is often restricted in some movements and in the size of spaces that can be accessed

* Corresponding author. Fax: +1-443-482-2380.
  E-mail addresses: parker@serc.si.edu (G.G. Parker).
  [1] Fax: +1-541-758-7760. *E-mail address*: lefsky@fsl.orst.edu (M.A. Lefsky).
  [2] Fax: +1-301-614-6522. *E-mail address*: harding@denali.gsfc.nasa.gov (D.J. Harding).

without interference. In the extreme, the sensor itself (even the relatively compact quantum sensor) is limited in the sorts of spaces that might be reached.

The challenge of obtaining full coverage of canopy environments is potentially met by remote sensing sensors, especially laser altimeters. Unlike more familiar systems that primarily sense the outer canopy surface (e.g., Landsat TM, aerial photography), these devices can perceive internal structure throughout the canopy (Lefsky, Harding, Cohen, Parker, & Shugart, 1999). Particularly promising is the newer implementation of waveform-sampling laser altimeters, such as Scanning Lidar Imager of Canopies by Echo Recovery (SLICER), an airborne sensor that provides a vertically detailed view of canopy reflectance (at 1064 nm, near infrared) over small (e.g., 10 m) footprints (Harding, Blair, Garvin, & Lawrence, 1994; Harding, Blair, Rabine, & Still, 2000; Harding, Lefsky, Parker, & Blair 2001; Lefsky, Cohen, et al., 1999; Lefsky, Harding, et al., 1999). Since canopy properties of reflectance and transmittance are closely related, such an instrument could provide information on light environments at an ecologically interesting scale.

A remote sensing approach, such as that of laser altimeters, could overcome many of the restrictions of in-situ measurements and quantify the pattern of radiation in canopies rapidly with wide spatial coverage. Our objectives in this study were to: (1) compare the transmittance pattern of different canopy types derived from in-canopy measurements with light sensors and those from SLICER waveforms; (2) assess the applicability of such a comparison across several forest types and stages; and (3) evaluate the capacity to capture small-scale variation in light environments. To make this comparison we took advantage of existing SLICER data acquired on missions to test its capacity to measure forest structure and other observations of canopy Photosynthetically Active Radiation (PAR) transmittance. This is an unplanned but fortuitous comparison between very different methods of deriving light transmittance profiles.

2. Methods

2.1. The study sites

Measurements were made both with SLICER and from the ground at five forest sites. Three were in eastern broadleaf forests on the Maryland coastal plain and the others were in old-growth Douglas fir forests in the Washington and Oregon Cascades. The eastern stands are part of a chronosequence study at the Smithsonian Environmental Research Center (SERC) and represent distinct stages in canopy development of the tulip poplar forest association described by Brush, Lenk, and Smith (1980). These stand are characterized by tulip poplar (*Liriodendron tulipifera* L.), but also have sweetgum (*Liquidambar styraciflua* L.), several species of oaks and hickories (*Quercus* L. and *Carya*

Nutt.), and American beech (*Fagus grandifolia* Ehrh.) dominant at different developmental stages. At the time of measurement, the young stand ("cornside") was a 20-year-old stand with an elevated monomodal canopy 18 m in maximum height; the intermediate stand ("Contee's") was 45 years old with a broad overstory to 32 m and a slight understory; and the mature stand ("tower"), about 105 years old, had a bimodal canopy and a maximum height of 40 m. These stands, at slightly earlier stages, were described by Brown and Parker (1994) and Parker, O'Neill, and Higman (1989). The forest at the Wind River Canopy Crane Research Facility ("Wind River") is about 400–500 years old. The tallest tree is 67 m and the canopy is estimated to be monomodal with maximum leaf area density in the lower third of this height (Parker, 1997; van Pelt & North, 1996). This stand was described by DeBell and Franklin (1987) and Franklin and DeBell (1988). The forest studied at the H.J. Andrews Experimental Forest ("HJA") in the central Oregon Cascades was an approximately 250-year-old stand on the terrace of a mountain creek. The maximum height of this stand was estimated to be 71 m from diameter measurements and regressions of top height and diameter from Garman, Acker, Ohmann, and Spies (1995). HJA is an intensive site for forestry, hydrology, and ecological research (van Cleve & Martin, 1991). Both of the western forests are dominated by Douglas fir (*Pseudotsuga menziesii* (Mirb.) Franco) and western hemlock (*Tsuga heterophylla* (Raf.) Sarg.).

2.2. Remote observations

Laser altimeter or light detection and ranging (lidar) sensors have been used to obtain accurate high resolution measurements of terrestrial surface elevations from airborne (e.g., Blair & Hoften, 1999; Bufton, 1989; Krabill, Collins, Link, Swift, & Butler, 1984), space shuttle (Garvin et al., 1998), and, soon, satellite (Dubayah et al., 1997) platforms. The first lidar sensors employed to study vegetation recorded the distance to the first reflective surface intercepted by a laser pulse over a relatively small sampling area, or footprint, usually less than 1 m in diameter (Arp, Griesbach, & Burns, 1982; Ritchie, Everitt, Escobar, Jackson, & Davis, 1992; Schreier, Logheed, Gibson, & Russell, 1984; Weltz, Ritchie, & Fox, 1994). When distances measured to the top surface of a canopy were compared with corresponding measurements to the forest floor (obtained through gaps in the canopy), the height of dominant trees was inferred. Similar techniques have been used to predict canopy height, timber volume and forest biomass (Maclean & Krabill, 1986; Naesset, 1997; Nelson, Krabill, & Tonelli, 1988), canopy cover (Ritchie, Evans, Jacobs, Everitt, & Weltz, 1993; Weltz et al., 1994), and aerodynamic roughness (Menenti & Ritchie, 1994).

The new generation of lidar instruments developed at NASA's Goddard Space Flight Center (Blair, Coyle, Bufton, & Harding, 1994; Blair & Hoften, 1999; Blair, Rabine,

& Hofton, 1999; Bufton, 1989; Bufton et al., 1991; Dubayah et al., 1997; Garvin et al., 1998) have extended this measurement capability. Whereas earlier devices sampled the distance to the first reflective surface over a small footprint, the newer devices transmit a pulse that covers a larger footprint (10 m diameter and larger) and record the timing and power (i.e., the waveform) of all backscattered light (Harding et al., 2001). This innovation provides additional information about surfaces below the top of the canopy. Although the power of the return signal attenuates with depth into the canopy, a return of energy from the ground is identifiable in nearly all footprints — this allows an estimate of the total height of the stand within the footprint, and indicates that some energy is available for the detection of understory foliage. The lidar waveform can be transformed to estimate the whole canopy transmittance and the vertical distribution of reflective surfaces (the "canopy height profile"; Harding et al., 2000; Lefsky, 1997). In this study, we used information from the SLICER device. A technical description of the SLICER device is provided in Harding et al. (2000) and a validation of the technique for measuring canopy height profiles in closed-canopy, broadleaf forests is described in Harding et al. (2001).

2.3. SLICER data collection

Lidar waveforms for both the eastern and western sites were collected by the SLICER instrument in September 1995. The data obtained over the eastern sites is described in Harding et al. (2001). The corresponding data for the western sites is similar in all but two ways. The SLICER system was configured to record waveforms from five scanning positions (footprints) across each transect. Examination of the data from the eastern sites indicated that decreased energy was collected from the outermost scanning positions, and these data were not used in further analyses. This effect was not observed in the western data sets and, therefore, data from all five scanning positions were used in deriving transmittance profiles. The differences in received energy for the outermost scanning positions is likely due to improved alignment between the laser transmitter scan pattern and the receiver field of view (Harding et al., 2000). Secondly, the vertical sampling resolution of the waveforms collected over all sites was 11.12 cm. For each laser pulse, 566 samples were collected downward from the highest canopy surface within the laser footprint, yielding backscatter energy extending 63 m below the canopy top. In the eastern sites, where stand height is usually less than 40 m, the height range sampled by the waveforms is adequate. In the western sites, the tallest stands exceed this height range and, therefore, the waveform record downward from the canopy top occasionally did not extend to the ground and was artificially truncated. Examination of the lidar and associated field data suggests that the truncation problem

affects only about 3% of the waveforms in the data set used here (Lefsky, Cohen, et al., 1999).

2.4. Field measurements

In all stands, vertical canopy transects of quantum flux measurements were taken using a Li-Cor quantum sensor (LI-190, Li-Cor, Lincoln, NE) at numerous points. This sensor responds to the number of photons in the range of 400–700 nm (PAR); its response is cosine-corrected and, as used, the field of view is hemispherical upward. We usually sampled points distributed on a rectangular grid on the forest floor (in the HJA stand, a long transect), but in the crane site, we used a polar sampling scheme to obtain roughly uniform coverage throughout the 2-ha area of the circle accessed from the crane. Horizontal interpoint distances of balloon transects varied with stand height: 5, 10, and 25 m in the cornside, Contee's, and tower stands; 10 m at HJA and from 30 to 50 m at Wind River. Observations were made under uniform, usually clear, skies, within 2.5 h of solar noon, which reduced the angular motion of the sun during each transect. Observations taken under shifting cloud conditions (broken skies) were not used.

In all but one of the canopies, the sensor was mounted level on the flat top of a balloon (Parker et al., 1996) and the level was checked regularly. The size of the balloon varied according to stand stature — from small (0.5 m^3 volume) in short canopies with small crowns to large (1.5 m^3) in the HJA. At Wind River, the sensors were mounted on a small, leveled platform suspended below the personnel hoist (base dimensions 1.3×1.3 m) of the tower crane (Parker, 1997).

Each irradiance value recorded with the balloon system was the mean of ten 0.4-s measurements taken at each height, averaged and stored with a Campbell 21X datalogger (Campbell Scientific, Logan, UT). At the crane site, the height of each measurement depended on the lifting velocity and the data rate; with the balloon system, it was controlled by the length of the cable. Height increment was 1 m when using balloons and 2 m from the crane. The minimum height was usually 2 m when using the balloons but was at the ground surface at the crane site.

We logged balloon light measurements in the canopy only when the balloon was level. Incorrect readings, such as those caused by a balloon tilting in the sheer zone, were identified and removed. A graph of irradiance against the cosecant of the solar elevation angle (calculated for each measurement from the time of day) helped in identifying suspect measurements from above the canopy, those inconsistently high or low for that time of day.

Each in-canopy observation of irradiance was standardized to the corresponding outside measurement, yielding transmittance (T_{FIELD}, a relative illuminance in the sense of Yoda, 1978). For balloon transects that ascended to above-canopy locations, we used the topmost reading as the external value, in other cases it was estimated as previously described. We attempted to make each transect ascend to

well above the local canopy height; however, transects of balloon measurements differed in their maximum heights for various reasons (e.g., obstacles, gusting wind). In transects where the topmost observation was above the local canopy height but not as tall as the maximum for that site, we appended values of full transmittance ($= 1.0$) for heights up to the maximum for that site; this was not done for transects ending below the local top.

2.5. Calculating transmittance for SLICER waveforms

The calculation of transmittance from the SLICER waveforms is similar to the calculation of canopy height profiles (e.g., Harding et al., 2001; Lefsky et al., 1997), but without the adjustment for the shielding of far surfaces by near ones (the MacArthur–Horn transformation). The following steps are involved. First, the background noise level was calculated and removed from each waveform. Negative values resulting from this step — where variance in the noise caused the waveform signal to be less than the mean noise — were set to zero. Second, the ground return of each waveform was located and the ground elevation defined as the maximum elevation of the ground return. The ground return was subtracted from the waveform, which resulted in the return signal due to canopy components. Next, the power of the canopy return was accumulated downward from the top of the canopy, and was normalized by the total power in the waveform (canopy plus ground). The power of the ground return distribution was multiplied by a reflectance factor of 2, from Lefsky, Harding, et al. (1999), yielding its total power. Such normalized cumulative power distributions (NCPDs) are equivalent to the closure distribution of Harding et al. (2001) and can be averaged, using the ground as the reference elevation. In averaging these distributions, the cumulative power above the topmost canopy height was set to zero. Transmittance was then estimated from the averaged NCPD as follows (Eq. (1)):

$$T_{SLICER}(h) = 1 - NCPD(h + 1), \qquad (1)$$

where $T_{SLICER}(h)$ is the SLICER estimate of transmittance at height h and the NCPD($h + 1$) is the NCPD at height $h + 1$. We assume the contribution of multiple scattering to signal delay is small, as in Harding et al. (2000). The estimation of transmittance profiles from reflected energy does not explicitly account for canopy absorption of laser light. Since transmittance is equal to one minus the sum of cumulative reflectance and absorptance, the previous equation may be replaced with (Eq. (2))

$$1 = T + (1 + c)R, \qquad (2)$$

where c is the absorptance to reflectance ratio. At the 1064 nm laser wavelength, this ratio is nearly constant for canopy elements of various kinds. Moreover, absorptance by both needle and laminar foliage is low at this wavelength, typically in the range of 0.01–0.1 (e.g., Baldini, Fascini,

Nerozzi, Rossi, & Rotondi, 1997; Knapp & Carter, 1998; Williams, 1991). Thus, we believe the difference between T_{SLICER} and T_{FIELD} is small at this wavelength.

2.6. Characteristic points of transmittance profiles

We defined several aspects of a transmittance profile with potential functional significance. The height at which transmittance was 0.98 (h_{98}) is taken to indicate the canopy "radiation-effective" height, since we believe that 2% attenuation is a level that reliably indicates light has been intercepted. Slopes of the transmittance profile were estimated by calculating the bin-to-bin difference in mean transmittance, which was then smoothed using a five-bin boxcar window. The maximum slope of the profile we termed the "lumicline" (following Parker, 1997) and its height in the canopy, the lumicline height (h_{lum}). The height of the maximum variance in transmittance is called h_{varmax} and the height where transmittance falls to half the outside value is the half-height (h_{50}). The transmittance at the lowest level is the bulk transmittance (T_{bulk}).

2.7. Three-dimensional array

A three-dimensional data set of transmittance values was created for a 100×150-m section of the Wind River crane stem-map area, at the intersection of three different SLICER transects. The intersection area was larger than the 50-m width of each transect, with variable spacing between waveforms, often less than the 10-m separation of waveforms in individual transects. The locations of 270 SLICER waveforms were resampled to a 5-m grid using a nearest-neighbor criteria. Waveforms were then transformed to give estimates of the vertical distribution of transmittance, and these were inserted into a three-dimensional array.

2.8. Geostatistics

To summarize spatial pattern in transmittance for each height, isotropic semivariograms were created at two sites: the portion of the Wind River used to create the three-dimensional array and the area near the mature (tower) stand at SERC. At both sites, semivariograms for fractional transmittance were calculated for each 1 m high interval in the canopy. For the Wind River site, the same 270 waveforms used to create the three-dimensional array were used. At the SERC tower site, 464 waveforms from four intersecting SLICER transects were used. Semivariograms were created using the methods described in Isaaks and Srivastava (1989). A distance matrix was generated using the Universal Transverse Mercator (UTM) coordinates of each waveform, and the semivariance of unique pairs of waveforms were grouped into 1-m wide lag distance bins. Preliminary analysis indicated that semivariances and nugget variances were unrealistically low at lag distances less than 2 m, prob-

Table 1
The number of SLICER waveforms and field profiles of PAR used to compute average transmittances at each site

Stand	SLICER waveforms	PAR profiles	Date of PAR profile
Cornside	16	10	10/1996
Contee's	24	18	9/1998
Tower	12	29	6–7/1993
HJA	32	18	6/1996
Wind River	395	16	7/1995

Also given are the dates of the field measurements (all SLICER observations were taken September 1995).

ably due to the overlap between the footprints of the SLICER waveforms. To counter this, we regrouped all data from 0- and 4-m lag distance into a single-distance bin. The semivariance at each lag d ($y(d)$) was calculated as (Eq. (3))

$$y(d) = \frac{1}{2N(d)} \sum_{d}^{d_{\max}} [T_i - T_j]^2,$$ (3)

where the T_i and T_j are the transmittance at locations i and j and the sum is evaluated over all possible distances corresponding to that lag bin. A number of models for

describing the variograms were evaluated at both sites; the exponential model provided the best fit. It is given by (Eq. (4)):

$$y(d) = c_0 + c_1(1 - e^{(3d/a)}),$$ (4)

where $y(d)$ is the semivariance at lag d, c_0 is the nugget variance, $c_0 + c_1$ is the sill variance, and a is the range (Jongman, Ter Braak, & Van Tongeren, 1995). We use the practical range, the distance at which the variogram reaches 95% of the sill variance, as defined by Isaaks and Srivastava (1989). The nugget and sill variance, and the semivariogram range are descriptors of the minimum measurable variation, the total variation, and the distance at which the semivariance reaches the level of the general variance, respectively.

2.9. Comparison of mean transmittances

SLICER and field transmittance profiles were compared at each site by product–moment correlation and by testing the significance of the difference between the distribution of transmittance values for each height interval. Because transmittances at a given height are not normally distributed, the nonparametric robust rank-order test (Siegel, 1956) was used to compare the mean SLICER estimates of transmit-
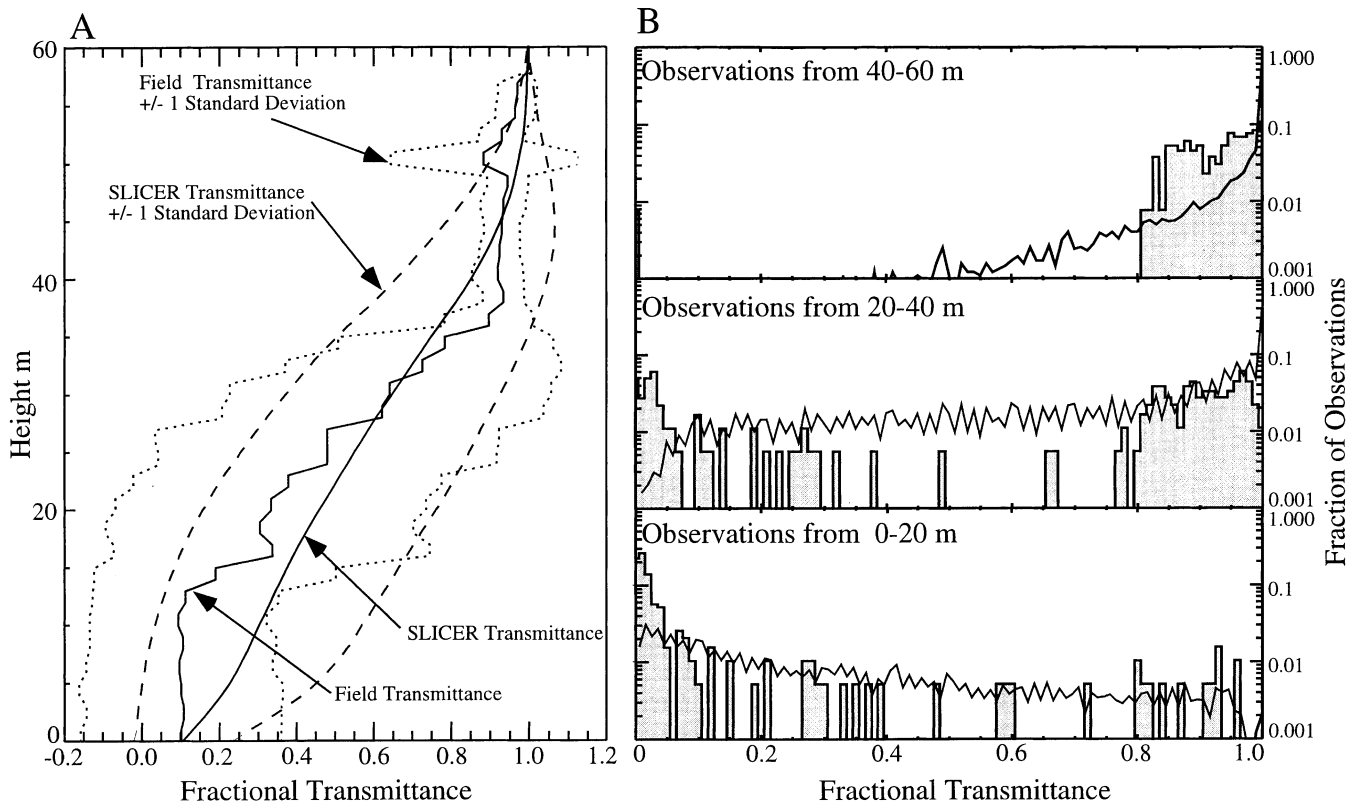

Fig. 1. Comparison of the field and SLICER estimates of the vertical transmittance profile for the Wind River site. In panel A, each estimate of the mean transmittance vertical profile is presented as a solid line. One standard deviation intervals are presented as dashed (SLICER) and dotted (field) lines. Panel B presents the distribution of SLICER (solid line) and field (shaded bars) observations in each of three height intervals above the ground (0–20, 20–40, and 40–60 m). Note the logarithmic scale of the vertical axis.

tances and the corresponding mean field measurements. The height interval used for the comparisons was 1 m, conforming to those of the field measurements — except at Wind River, where 2 m was used.

2.10. The data sets

The number of vertical profiles and waveforms used to compute mean transmittance profiles was roughly the same in all stands, except at the Wind River site where numerous waveforms were acquired in the same area as the dispersed field measurements (Table 1). Additional waveforms were acquired at the eastern tower site, but these others were not coincident with the field observation plot and are not used for comparison of transmittances. The SLICER and field measurements to be compared were spatially coincident except for the HJA stand. In the eastern stands, the field measurements were taken in the same plots used to validate the SLICER measure of canopy structure (Harding et al., 2001) and at Wind River, both sets of measurements were dispersed over the same area. However, at the HJA site, no lidar data were available for the field measurement plot. However, field measurements were made within a large, mostly intact, old-growth stand. Lidar observations were taken from within a contiguous section of the stand,

approximately 800 m from the field measurement site. All SLICER waveforms were acquired in September 1995; the field observations were taken at different times (Table 1).

3. Results

3.1. Comparison of profile statistics

Frequency distributions of transmittance were clearly asymmetrical and changing vertically in shape at all the sites, as indicated in Fig. 1 for the Wind River. In the upper layers of the canopy, transmittance was predominantly high, with some occasional low values (negative values of the skewness index — Fig. 1B, top panel) while in the lower canopy layers transmittance was generally very low, with occasional high values (positive values of skewness — Fig. 1B, middle and bottom panels). The curves of T_{SLICER} were similar in distribution to those of T_{FIELD}, but they were much smoother.

Comparison of field and SLICER estimates of several statistics of the vertical transmittance profiles show notable similarities for individual stands and consistent differences between eastern and western stands (Fig. 2). Both methods preserved the outer canopy curvature in the eastern stands
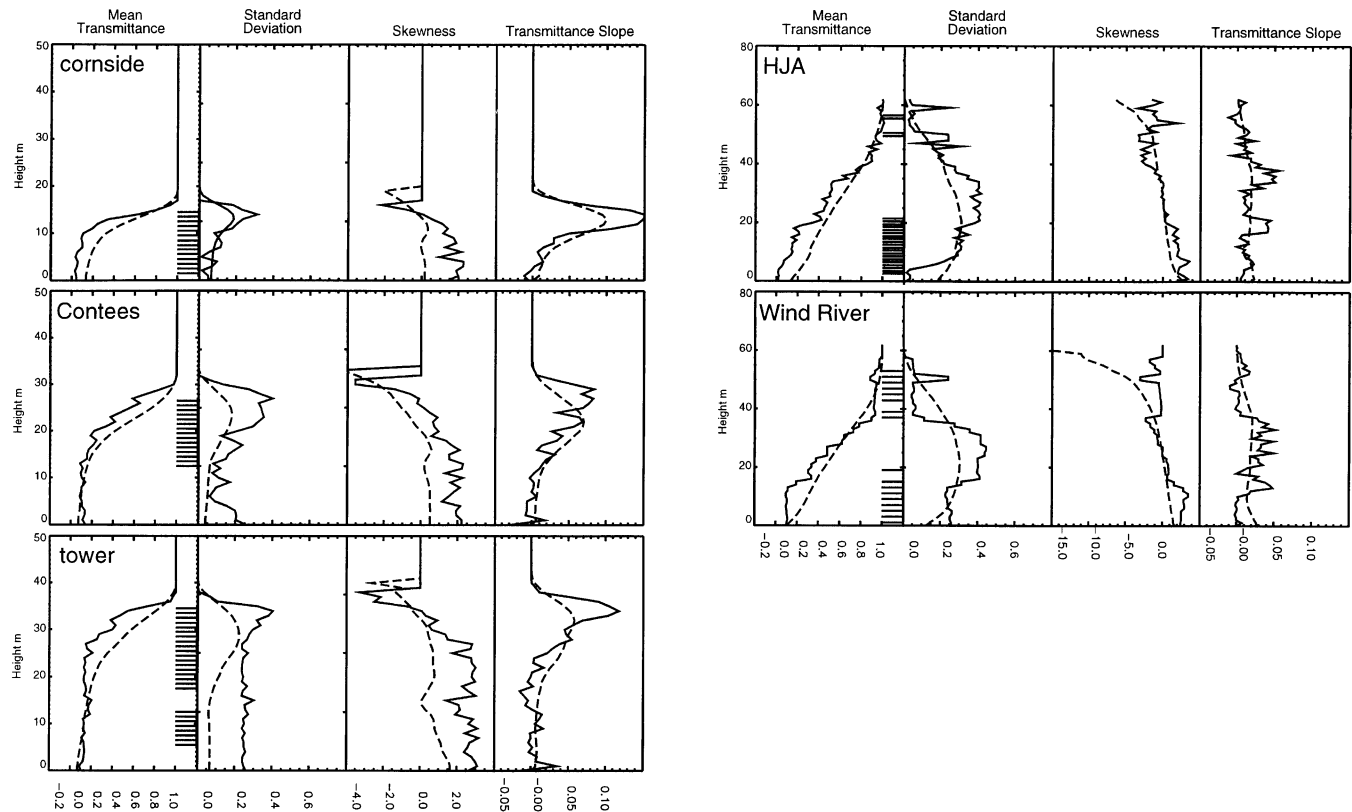

Fig. 2. Comparison of field and SLICER estimates of the vertical profile of transmittance for all five study areas. For each site, the three leftmost panels present the mean, standard deviation and skewness of the transmittance distributions as a function of height. The rightmost panel presents the bin-to-bin slope of the transmittance profile. Solid lines are field estimates and dashed lines are SLICER-derived. The dashes at the right of the first panel indicate heights where the mean transmittances differed significantly between methods.

Table 2
Significant points of the transmittance profiles as estimated from SLICER and field observations

	Cornside		Contee's		Tower		Wind River		HJA	
	SLICER	Field	SLICER	Field	SLICER	Field	SLICER	Field	SLICER	Field
Maximum slope, m^{-1}	0.10	0.15	0.07	0.08	0.06	0.12	0.03	0.05	0.02	0.06
h_{lum}	13	14	22	29	32	34	17	33	10	38
h_{varmax}	12	13	23	26	28	33	20	25	20	29
h_{98}	17	16	30	30	38	37	50	57	50	67
h_{50}	12	13	21	24	28	33	22	27	22	30
T_{bulk}	0.13	0.03	0.07	0.08	0.07	0.09	0.11	0.10	0.13	0.01

The lumicline (h_{lum}) is where the rate of attenuation is greatest. Significant heights in the canopy include the height of the greatest variability in transmittance (h_{varmax}), where transmittance falls to 0.98 (h_{98}) and 0.50 (h_{50}). The overall transmittance of the canopy observed near the ground is the bulk transmittance (T_{bulk}).

and the nearly linear profiles in the western ones. The product–moment correlation between the two transmittance estimates was high and significantly different from zero (all $P < .001$) at all sites ($r = .98, .92, .93, .98,$ and $.99$ for cornside, Contee's, tower, Wind River, and HJA, respectively). However, half of the height comparisons of mean transmittance differed significantly between methods based on the rank-order test. The general pattern of horizontal variability in transmittance (expressed as the standard deviation) was captured similarly by both methods. In the eastern stands, variability peaked in the upper canopy but in the western stands was elevated over a broad range of heights. However, in the tower stand the field measurements of variability were greater in the lower canopy than for SLICER. The skewness measure, reflecting the shape of the distribution of transmittance values, changed progressively from positive in the understory to negative in the upper canopy. Both methods captured this pattern, although in the outer canopy individual observations caused aberrant values in calculated skewness. Finally, the vertical pattern in the change in the mean transmittance, an indication of light absorption, was also consistent between methods, preserving the marked peak in the outer canopy for the eastern stands and the broad mode throughout the canopy for the western ones. The correlation between vertical change in transmittance and its horizontal variability calculated using T_{SLICER} was high at all sites ($r = .96, .97, .93, .84,$ and $.85$ for cornside, Contee's, tower, Wind River, and HJA, respectively).

3.2. Comparison of profile characteristics

Many characteristics of the mean transmittance profile were similarly estimated by both methods (Table 2). The maximum slope (change in transmittance per unit height) was within $0.06 \ m^{-1}$ between methods for all stands; the height of this zone (h_{lum}) agreed to within 7 m in the eastern stands, but not in the western ones. More similar between methods was the height of the greatest variability, h_{varmax}, which agreed to within 9 m in all stands, eastern and western. Heights of median transmittance, h_{50}, were within 8 m in all stands but HJA. The radiation-effective height,

h_{98}, of the canopy was similar between methods for the eastern stands but differed by 7 and 17 m with SLICER in Wind River and HJA, respectively. The bulk canopy transmittances, T_{bulk}, were within 0.10 in the eastern stands. In the western stands, the similarity between estimates varied widely: at Wind River it was very close (difference of 0.01), but at HJA it was not (difference of 0.12). SLICER remote estimates can differ from field measurements of canopy bulk transmittance by as much 10% (eastern stands) and 12% (western).

3.3. Vertical transmittance along horizontal transects

An example of the spatial variation of transmittance along 800 m transects is given in Fig. 3 for the Wind River (upper panel) and tower sites (lower panel). Note the footprint-to-footprint variation in pattern of transmittance: dark locations with maximum attenuation high in the canopy can be adjacent to places where high light reaches
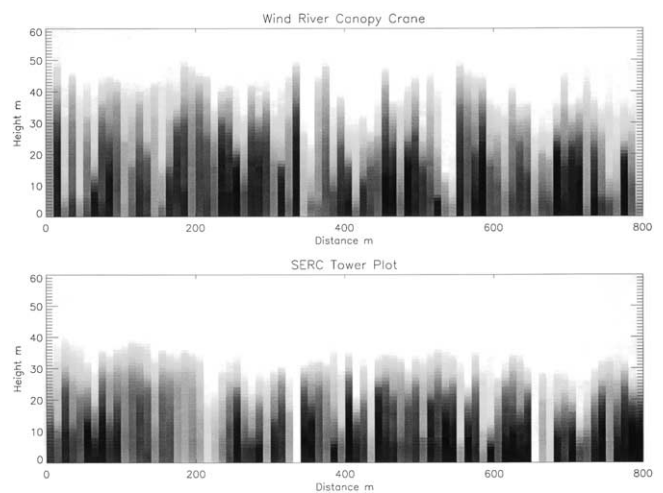

Fig. 3. Vertical pattern of canopy PAR transmittance in 800-m SLICER transects for forests at Wind River (top panel) and the SERC tower site (bottom panel). Ground elevations have been subtracted from each vertical profile, so the height refers to the local canopy height. Dark shading indicates low transmittance and light shading is for high transmittance. The shading scale is the same for both panels.

nearly to the ground. In both transects, such bright footprints correspond to spaces between trees — in the eastern stands, these are usually canopy gaps. Note also how the transects not only reflect the difference in the general stature of these stands but also illustrate, at a 10 m scale, the undulating surface of the outer canopy.

3.4. Transmittance in three dimensions

Fig. 4 presents several views of transmittances from selected heights from the three-dimensional array of transmittance values at Wind River. Transmittance values decreased as expected from the top of the canopy to the forest floor, as displayed in the left panel of Fig. 4. In the subsequent panels, the contrast of transmittance values at each height is expanded (through histogram equalization) to emphasize the spatial pattern within each level. The spatial pattern of transmittance was similar throughout the lower portion of the canopy, but changed dramatically between 45 and 60 m, with a large variation due to the tops of the dominant and codominant trees.

3.5. Spatial covariation

The minimum measurable variation (semivariogram nugget), the total variation (sill), and the correlation distance (range) of the spatial pattern of transmittance varied with height at both the Wind River and tower sites (Fig. 5). The vertical profiles of both the nugget and sill variance resembled the profiles of the standard deviation of transmittance (Fig. 2). At the tower site, both components of variance peaked relatively high in the canopy (66% of effective height); both components peaked lower (45% of height) at Wind River.

The range of the semivariograms generally increased with height at both sites. In the eastern site, the range was approximately 20 m in the zone between the forest floor and 20 m in height. Above 20 m, the range increased to 50 m between 20 and 30 m, and then abruptly declined above 35 m height. There was a similar pattern in the western site. The range was low (15–20 m) for heights from 10 to 40 m. Above this level, the range rapidly increased to 60 m at a height of 43 m and then declined
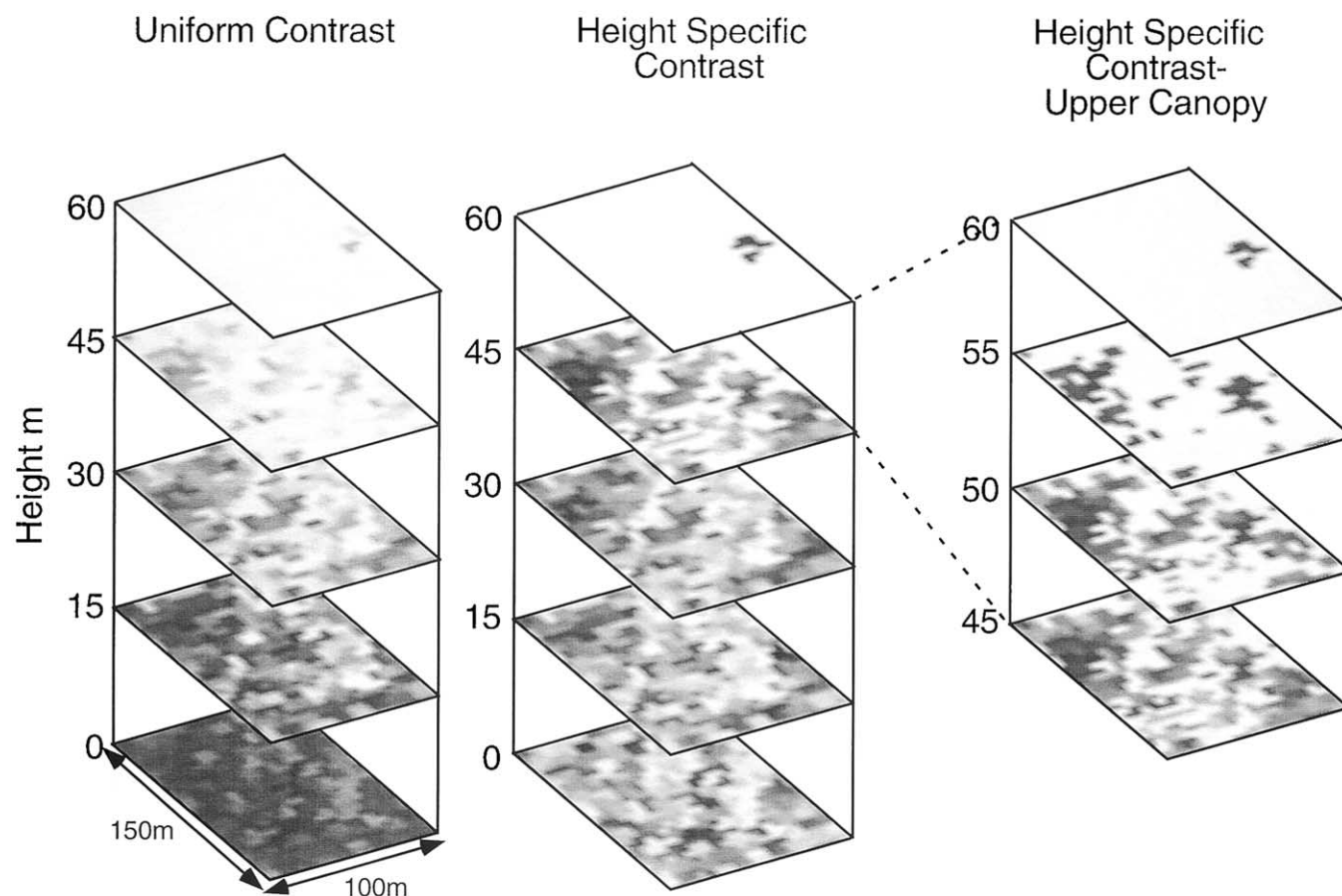

Fig. 4. Volumetric transmittance in a 100 × 150-m section of the Wind River site. Dark shading indicates low transmittance and light shading indicates high transmittance. The left panel gives the general pattern as a stacked series of plots separated by 15 m, using a uniform relation between shading and transmittance at all levels. To emphasize the spatial pattern of transmittance at each level, a histogram-equalized relation of shading and transmittance for all height levels is given (middle panel) and, for detail, the layers between 45 and 60 m (right panel).
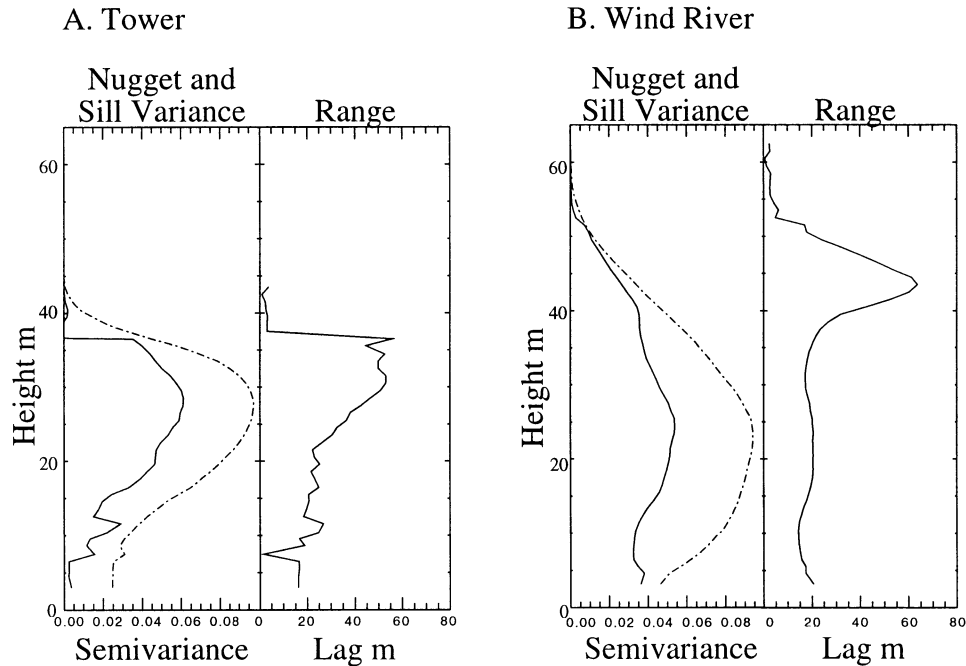
A. Tower

B. Wind River

Fig. 5. Vertical pattern in the geostatistics of light penetration at the tower (A) and Wind River (B) from parameters of semivariograms fitted to SLICER data. For each site, the nugget (solid line) and sill variance (dashed line) are given in the left panel and the range of the semivariogram is in the right panel.

to nearly zero at the top of the canopy. In both stands, the maximum range was closer to the top of the canopy than were either the maximum sill or nugget variances, and in both cases, the maximum range was associated with the top of the vertical space occupied by the crowns of the dominant and codominant trees.

4. Discussion

We have compared how a novel remote sensing technology and field measurements can reveal a functional attribute of vegetation and have also described some new observations of this function. Below, we describe the methodological considerations that might have influenced the comparison and then discuss some general characteristics of light transmittance in forest canopies, as seen by SLICER.

4.1. Differences between methods

One possible source of differences between methods was the lag between observations. However, these canopies probably changed little in the interval between measurements — they grew little and suffered no disturbances. Except for the comparison at the HJA forest, where SLICER and field observations were separated by 800 m, the spatial registration of the two sorts of measurements was very close. Even in the HJA case, however, the forest type is homogeneous over this area and many of the

estimated attributes of the transmittance profiles were similar between methods.

Many differences in the two sensing systems influenced the comparison of derived transmittances. SLICER is sensitive to the energy of monochromatic (1064 nm) radiation reflected from canopy surfaces to a very narrow field of view at the zenith, while the field sensor system responds to the number of quanta in a broad wavelength band (400–700 nm) downwelling over a hemispherical view. The two methods can produce profiles of differing smoothness; the transmittance profile derived from SLICER is monotonic by definition (Eq. (1)), whereas field measurements may show reverses due to local light flecks and other openings. This difference could affect the statistical similarity of transmittances at some within-canopy levels. While the absolute transmittance and reflectance of foliage tissues differed in the wavelengths perceived by the two systems, the ratio of transmittance to reflectance (T:R) was near 1 in both the visible (0.15:0.15) and near infrared (0.45:0.45). The field method senses transmittance directly whereas the SLICER instrument indicates transmittance plus absorptance. However, since absorptance in the near infrared is small and likely constant, this difference is also likely to be small.

The agreement between the vertical profiles of transmittance from the two methods was better for the eastern sites than for those in the west. Differences in canopy organization in these stands likely affect the variability of depths to which light from different angles can penetrate. The outer canopies of the eastern deciduous stands are more spatially homogenous in the horizontal plane than those of the western sites

— the individual eastern crowns are broader and much more likely to adjoin neighbors than the narrower, more isolated crowns of the west. In the western stands, sunlight incident at a typical elevation angle would pass through several crowns before intercepting the forest floor, whereas the overhead SLICER illumination can penetrate farther down in the large spaces between adjacent crowns. Thus, the SLICER method would tend to overestimate transmittance near the forest floor compared with field observations, which was observed in this comparison. In the eastern stands, this effect would be minimized, because deep spaces between trees are less common. The bias of SLICER estimates of transmittance would likely increase with increased variability in the upper canopy surface (e.g., noncontiguous crowns, open forests, disturbed situations) and with increasingly lower sun elevation angles (e.g., high-latitude forests).

The SLICER estimates of transmittances involve a source of illumination that is directed from the zenith, whereas the sun is rarely directly overhead, and even then, only between the tropics. This problem could be addressed if the lidar device were aimed at various angles of actual solar illumination — the waveforms returned from such orientations would better reflect interaction with canopy elements along the path of direct sunlight — a similar approach was used by Vanderbilt, Bauer, and Silva (1979) to estimate solar irradiance in a wheat canopy. A second method to address this problem would be to collect lidar data at a nadir orientation over a large area, creating a three-dimensional array like that presented in Fig. 4. The path that a direct beam of sunlight would take through this grid could be calculated and the transmittances along the path could be accumulated to more accurately estimate the transmittance at any point for which the path fell entirely within the grid. The individual transmittance at any point would still be collected at the nadir orientation, but the influence of coarse-scale canopy heterogeneity would be more accurately simulated. This approach should be feasible using data from the wide-swath Laser Vegetation Imaging Sensor (Blair, Rabine, et al., 1999) device — however, such an approach was not feasible using the spatially limited data sets available for this study.

4.2. Transmittance average, variability, and spatial covariance

Semivariograms (Fig. 5) summarize spatial aspects of horizontal patterns in transmittance from the two sites illustrated as transects in Fig. 3. In both cases, the range of the semivariogram is highest in the upper canopy (where it likely reflects the large spaces between crowns) and declines with depth in the canopy (probably paralleling the smaller intercrown spacing in the midcanopy). Below this level, the range declines sharply, possibly reflecting the relative scarcity of intercrown spaces. It is possible that this represents an inversion of causes, from a pattern dominated by open spaces in the upper canopy to one dominated by plant material in the lower canopy.

The capacity to capture this spatial variation has implications for how various canopy functions are perceived and modeled. Many canopy functions related to light derive from the pattern of attenuation. For example, the extent to which PAR light is absorbed in canopies has been used to predict primary production in vegetation (Cannell, Milne, Sheppard, & Unsworth, 1987; Linder, 1985; Monteith, 1977, 1994) and is the basis of models of local (e.g., Gutschick, 1991), regional, and global (e.g., Field, Behrenfeld, Randerson, & Falkowski, 1998; Running et al., 1999) production. The location of this activity and its variation are important for assessment of habitat quality and environmental heterogeneity.

The vertically variable pattern in spatial covariance of canopy structure such as we describe may help in the interpretation of two-dimensional remotely sensed images. Cohen, Spies, and Bradshaw (1990) used geostatistics to characterize stand structural complexity of Douglas fir forests derived from 1 m resolution aerial videography. In that work, the maximum ranges found were from 8 to 18 m, considerably less than the 60-m range we observed at the Wind River site. While some of this difference is related to real canopy variation between the sites, we suspect that most is due to fundamental differences in the sensing approaches. Spatial patterns at a variety of height levels are mixed in images. The large-scale variability of the upper canopy surface is superimposed upon the smaller-scale variability of the lower canopy. Correspondingly, the spatial statistics calculated from conventional two-dimensional images are averages of the actual spatial structure of the canopy at many levels. Consequently, these statistics do not reflect the actual spatial structure of the canopy at any one height level. Such a distinction may be important for certain applications such as the estimation of the surface roughness of canopies for atmospheric modeling.

5. Conclusions

The SLICER sensor provides a view of canopy light environments that was not previously available. It depicts the average pattern and yields the vertical profiles of important statistical moments and several summary characteristics of PAR transmittance profiles measured directly within the canopy in a range of forest types and development stages. Moreover, the SLICER system sensed canopy transmittance not only with a broader coverage but also at a finer spatial scale than practical for in-canopy observations, providing a summary of the volumetric distribution of light environments. Mean canopy transmittance profiles reflected forest type — the western sites had nearly linear declines in transmittance with height while in the eastern ones the attenuation was greatest in the upper canopy. Horizontal variation was highest where transmittance changed most rapidly with height. Horizontally within a height, transmittances were nonnormally distributed, with a marked change

from negative skewness in the overstory to positive skewness in the understory. The spatial scale of horizontal variability was greatest in the overstory and least in the understory. The canopy feature affecting spatial covariance in transmittance may shift from the organization of open spaces, in the upper canopy, to the locations of crowns, in the understory. Finally, the capacity to assess this canopy attribute at a small spatial scale has important implications for the estimation of environmental diversity, carbon acquisition, and forest growth at large scales. This work used data sets that were fortuitously spatially coincident but were not systematically collected for the purpose of comparing transmittance profiles. A well-planned experiment that collects temporally and spatially coincident lidar and in-situ observations in a diverse set of stand types could assess the wider potential of waveform lidar to measure canopy transmittances.

References

Arp, J. D., Griesbach, J. C., & Burns, J. P. (1982). Mapping in tropical forests: a new approach using the laser APR. *Photographic Engineering*, *48*, 91–100.

Baldini, E., Fascini, O., Nerozzi, F., Rossi, F., & Rotondi, A. (1997). Leaf characteristics and optical properties of different woody species. *Trees*, *12*, 73–81.

Blair, J. B., Coyle, D. B., Bufton, J. L., & Harding, D. J. (1994). Optimization of an airborne laser altimeter for remote sensing of vegetation and tree canopies. *Proceedings of IGARSS'94*, *II*, 939–941.

Blair, J. B., & Hoften, M. A. (1999). Modeling laser altimeter return waveforms over complex vegetation using high-resolution elevation data. *Geophysical Research Letters*, *26*, 2509–2512.

Blair, J. B., Rabine, D. L., & Hofton, M. A. (1999). The laser vegetation imaging sensor: a medium-altitude, digitisation-only, airborne laser altimeter for mapping vegetation and topography. *ISPRS Journal of Photogrammetry and Remote Sensing*, *54*, 115–122.

Brown, M. J., & Parker, G. G. (1994). Canopy light transmittance in a chronosequence of mixed-species deciduous forests. *Canadian Journal of Forest Research*, *24*, 1694–1703.

Brush, G. S., Lenk, C., & Smith, J. (1980). The natural forests of Maryland: an explanation of the vegetation map of Maryland. *Ecological Monographs*, *50*, 77–92.

Bufton, J. L. (1989). Laser altimetry measurements from aircraft and spacecraft. *Proceedings of the IEEE*, *77*, 463–477.

Bufton, J. L., Garvin, J. B., Cavanaugh, J. F., Ramos-Izquierda, L., Clem, T. D., & Krabill, W. B. (1991). Airborne lidar altimetry for profiling of surface topography. *Optical Engineering*, *30*, 72–78.

Cannell, M. G. R., Milne, R., Sheppard, L. J., & Unsworth, M. H. (1987). Radiation interception and productivity of willow. *Journal of Applied Ecology*, *24*, 261–278.

Cohen, W. B., Spies, T. A., & Bradshaw, G. A. (1990). Semivariograms of digital imagery for analysis of conifer canopy structure. *Remote Sensing of Environment*, *34*, 167–178.

DeBell, D. S., & Franklin, J. F. (1987). Old-growth Douglas-fir and western hemlock: a 36-year record of growth and mortality. *Western Journal of Applied Forestry*, *2*, 111–114.

Dubayah, R., Blair, J. B., Bufton, J. L., Clark, D. B., JaJa, J., Knox, R., Luthcke, S. B., Prince, S., & Weishampel, J. (1997). The vegetation canopy lidar mission. In: *Land satellite information in the next decade: II. sources and applications* (pp. 100–112). Washington, DC: ASPRS.

Ellsworth, D. S., & Reich, P. B. (1993). Canopy structure and vertical patterns of photosynthesis and related leaf traits in a deciduous forest. *Oecologia*, *96*, 169–178.

Field, C., & Mooney, H. A. (1986). The photosynthesis–nitrogen relationship in wild plants. In: T. J. Givnish (Ed.), *On the economy of plant form and function* (pp. 25–55). Cambridge: Cambridge Univ. Press.

Field, C. B., Behrenfeld, M. J., Randerson, J. T., & Falkowski, P. (1998). Primary production of the biosphere: integrating terrestrial and oceanic components. *Science*, *281*, 237–240.

Franklin, J. F., & DeBell, D. S. (1988). Thirty-six years of tree population change in old-growth *Pseudotsuga–Tsuga* forest. *Canadian Journal of Forest Research*, *18*, 633–639.

Garman, S. L., Acker, S. A., Ohmann, J. L., & Spies, T. A. (1995). *Asymptotic height–diameter equations for twenty-four tree species in western Oregon*. Research Contribution 10 (22 pp.), OSU Forest Research Lab., Corvallis.

Garvin, J., Bufton, J., Blair, B., Harding, D., Luthcke, S., Frawley, J., & Rowlands, D. (1998). Observations of the Earth's topography from the shuttle laser altimeter (SLA): laser–pulse echo-recovery measurements of terrestrial surfaces. *Physics and Chemistry of the Earth*, *23*, 1053–1068.

Gutschick, V. P. (1991). Joining leaf photosynthesis models and canopy photon-transport models. In: R. B. Myneni, & J. Ross (Eds.), *Photon–vegetation interactions: applications in optical remote sensing and plant ecology* (pp. 501–535). Berlin: Springer-Verlag.

Harding, D. J., Blair, J. B., Garvin, J. G., & Lawrence, W. T. (1994). Laser altimeter waveform measurement of vegetation canopy structure. *Proceedings of IGARSS'94*, *II*, 1251–1253.

Harding, D. J., Blair, J. B., Rabine, D. L., & Still, K. L. (2000). *SLICER airborne laser altimeter characterization of canopy structure and sub-*

canopy topography for the BOREAS northern and southern regions: instrument and data product description. NASA Technical Memorandum NASA/TM-2000-209891.

Harding, D. J., Lefsky, M. A., & Parker, G. G. (2001). Laser altimeter canopy height profiles: methods and validation for closed-canopy, broadleaf forests. *Remote Sensing of Environment.*

Isaaks, E. H., & Srivastava, R. M. (1989). *An introduction to applied geostatistics.* New York: Oxford Univ. Press.

Jongman, R. H. G., Ter Braak, C. J. F., & Van Tongeren, O. F. R. (1995). *Data analysis in community and landscape ecology.* New York: Cambridge Univ. Press.

Knapp, A. K., & Carter, G. A. (1998). Variability in leaf optical properties among 26 species from a broad range of habitats. *American Journal of Botany, 85,* 940–946.

Krabill, W. B., Collins, J. G., Link, L. E., Swift, R. N., & Butler, M. L. (1984). Airborne laser topographic mapping results. *Photogrammetric Engineering and Remote Sensing, 50,* 685–694.

Lefsky, M. A. (1997). *Application of lidar remote sensing to the estimation of forest canopy and stand structure.* PhD dissertation, Department of Environmental Science, University of Virginia, Charlottesville, VA.

Lefsky, M. A., Cohen, W. B., Acker, S. A., Parker, G. G., Spies, T. A., & Harding, D. (1999). Lidar remote sensing of the canopy structure and biophysical properties of forests of Douglas-fir and western hemlock. *Remote Sensing of Environment, 70,* 339–361.

Lefsky, M. A., Harding, D. J., Cohen, W. B., Parker, G., & Shugart, H. (1999). Surface lidar remote sensing of forest basal area and biomass in deciduous forests of eastern Maryland, USA. *Remote Sensing of Environment, 67,* 83–98.

Linder, S. (1985). Potential and actual production in Australian forest stands. In: J. J. Landsberg, & W. Parsons (Eds.), *Research for forest management* (pp. 11–35). Melbourne: CSIRO Publishing.

Maclean, G. A., & Krabill, W. B. (1986). Gross merchantable timber volume estimation using an airborne lidar system. *Canadian Journal of Remote Sensing, 12,* 7–8.

Menenti, A., & Ritchie, J. C. (1994). Estimation of effective aerodynamic roughness of Walnut Gulch watershed with laser altimeter measurements. *Water Resources Research, 30,* 1329–1337.

Monteith, J. L. (1977). Climate and efficiency of crop production in Britain. *Philosophical Transactions of the Royal Society of London, Series B: Biological Sciences, 281,* 277–294.

Monteith, J. L. (1994). Validity of the correlation between intercepted radiation and biomass. *Agriculture and Forest Meteorology, 68,* 221–230.

Naesset, E. (1997). Estimating timber volume of forest stands using airborne laser scanner data. *Remote Sensing of Environment, 61,* 246–253.

Nelson, R., Krabill, W., & Tonelli, J. (1988). Estimating forest biomass and volume using airborne laser data. *Remote Sensing of Environment, 24,* 247–267.

Parker, G. G. (1995). Structure and microclimate of forest canopies. In: M. Lowman, & N. Nadkarni (Eds.), *Forest canopies — a review of research on a biological frontier* (pp. 73–106). San Diego: Academic Press.

Parker, G. G. (1997). Canopy structure and light environment of an old-growth Douglas-fir/western hemlock forest. *Northwest Science, 71,* 261–270.

Parker, G. G., O'Neill, J. P., & Higman, D. (1989). Vertical profile and canopy organization in a mixed deciduous forest. *Vegetation, 89,* 1–12.

Parker, G. G., Smith, A. P., & Hogan, K. P. (1992). Access to the upper forest canopy with a large tower crane. *BioScience, 42,* 664–670.

Parker, G. G., Stone, P. J., & Bowers, D. (1996). A balloon for microclimate observations in the forest canopy. *Journal of Applied Ecology, 33,* 173–177.

Ritchie, J. C., Everitt, J. H., Escobar, D. E., Jackson, T. J., & Davis, M. R. (1992). Airborne laser measurements of rangeland canopy cover and distribution. *Journal of Range Management, 45,* 189–193.

Ritchie, J. J., Evans, D. L., Jacobs, D., Everitt, J. H., & Weltz, M. A. (1993). Measuring canopy structure with an airborne laser altimeter. *Transactions of the ASAE, 36,* 1235–1238.

Running, S. W., Baldocchi, D. D., Turner, D. P., Gower, S. T., Bakwin, P. S., & Hibbard, K. A. (1999). A global terrestrial monitoring network integrating tower fluxes, flask sampling, ecosystem modeling and EOS satellite data. *Remote Sensing of Environment, 70,* 108–127.

Schreier, J., Logheed, L., Gibson, J. R., & Russell, J. (1984). Calibration of an airborne laser profiling system. *Photogrammetric Engineering and Remote Sensing, 50,* 1591–1598.

Siegel, S. (1956). *Nonparametric statistics for the behavioral sciences.* New York: McGraw-Hill.

Thompson, D. R., & Hinckley, T. M. (1977). Spatial and temporal variations in stand microclimate and the water status of several species in an oak–hickory forest. *American Midland Naturalist, 94,* 373–380.

van Cleve, K., & Martin, S. (1991). *Long-term ecological research in the United States — a network of research sites* (6th ed.). *LTER Publication, No. 11.* Seattle, WA: Long-Term Ecological Research Network Office.

van Pelt, R., & North, M. P. (1996). Analyzing canopy structure in Pacific Northwest Old-Growth forests with a stand-scale crown model. *Northwest Science, 70,* 15–31 (special issue).

Vanderbilt, V. C., Bauer, M. E., & Silva, L. F. (1979). Prediction of solar irradiance in a wheat canopy using a laser technique. *Agriculture and Forest Meteorology, 20,* 147–160.

Vose, J. M., Sullivan, N. H., Clinton, B. D., & Bolstad, P. V. (1995). Vertical leaf area distribution, light transmittance, and application of the Beer–Lambert law in four mature hardwood stands in the southern Appalachians. *Canadian Journal of Forest Research, 25,* 1036–1043.

Weltz, M. A., Ritchie, J. C., & Fox, H. D. (1994). Comparison of laser and field measurements of vegetation height and canopy cover. *Water Resources Research, 30,* 1311–1319.

Williams, D. L. (1991). A comparison of spectral reflectance properties at the needle branch and canopy level for selected conifer species. *Remote Sensing of Environment, 35,* 79–93.

Yoda, K. (1978). The three-dimensional distribution of light intensity in a tropical rain forest in West Malaysia. *Japanese Journal of Ecology, 24,* 247–254.